

Nucleon Structure Functions

F. Eisele

Physikalisches Institut der Universität Heidelberg

25th October 2018

Abstract

New structure function measurements from fixed target experiments and especially HERA are reviewed. The extraction of parton distributions from these measurements is discussed with special emphasis on systematic problems. New information from Drell-Yan and direct photon production experiments are also presented. Finally the present uncertainties of our knowledge on parton distributions and on α_s from DIS experiments are discussed ¹.

1 Introduction

Our knowledge of nucleon structure functions and of the parton distributions (PDF's) derived from them has steadily improved due to both the improvement of a large variety of measurements and a more sophisticated theoretical treatment of hard scattering processes in perturbative QCD. Structure functions and PDF's are needed for two reasons:

- They are a necessary input for all hard scattering processes involving nucleons to make precise predictions in the standard model and of course to look for deviations from these predictions, and to make predictions for signals and backgrounds at colliders especially the LHC.
- They contain important information about the underlying physics of hadrons and allow stringent tests of perturbative QCD.

A hard scattering process in a hadron hadron collision is shown in figure 1. Two partons with momentum fractions x_1 and x_2 scatter and produce a

¹Invited talk XVIII Physics in Collision

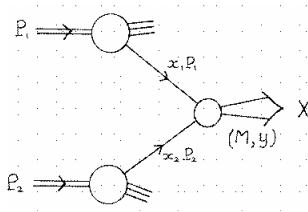


Figure 1: *Example of a LO hard scattering process in hadron-hadron scattering.*

heavy state with mass M which can be jets, γ +jet, heavy Bosons or Quarks or new particles like Higgs or SUSY. The differential parton-parton cross section $d\sigma_{ij}$ is given by pQCD, the total cross section is given by

$$d\sigma = \sum_{i,j} \int dx_1 dx_2 f_i(x_1, \mu^2) f_j(x_2, \mu^2) \star d\sigma_{ij}(p_1, p_2, \alpha_s(\mu^2), M_2/\mu^2)$$

where the sum goes over all parton flavours which contribute. In LO pQCD the cross section factorises into the parton luminosity which depends on the parton densities f_i, f_j and the differential parton-parton cross section. The parton densities are therefore universal to all hard scattering processes provided they are extracted in higher order (so far in NLO) and corrected to the leading order diagrams. The parton densities depend on the fractional momentum x and the typical scale μ^2 of the process.

Deep inelastic lepton nucleon scattering (DIS) is the basis for our knowledge of PDF's. The kinematic plane of available measurements in (x, Q^2) from fixed target and HERA experiments is shown in figure 2.

The data cover now a huge region

$$2 \star 10^{-5} < x < .75 ; 1 \text{ GeV}^2 < Q^2 < 40000 \text{ GeV}^2$$

where HERA has added 2 orders of magnitude in both variables. The kinematic plane for hard scattering processes at LHC (14 TeV) is compared in figure 3 where the mass M of the produced system is used as scale. Also shown are lines of constant rapidity y of the system M which is proportional to $(x_1 - x_2)$. It is obvious that due to the high CMS energy of LHC a very large fraction of interesting LHC physics is physics at low x (here taken as $x < 10^{-2}$) [1]. For example the production of Higgs particles in the mass

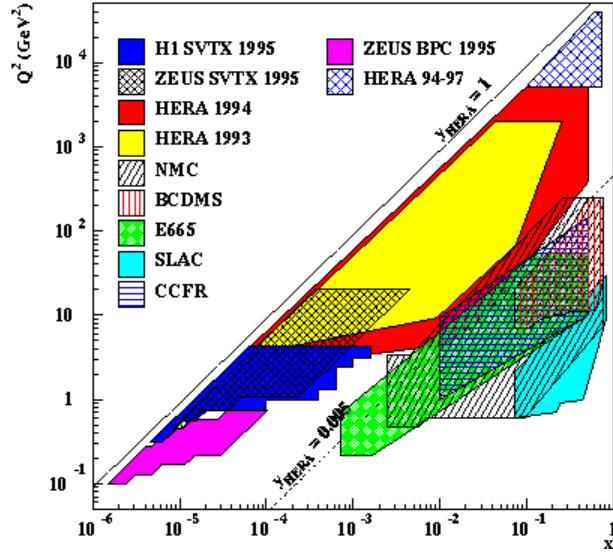


Figure 2: Available DIS data from fixed target and HERA.

range $100 \text{ GeV} < M_H < 500 \text{ GeV}$ in the rapidity range $|y| < 2.5$ requires the knowledge of the gluon density for x -values as low as 10^{-4} which is now available due to HERA.

In order to apply our present knowledge on PDF's we have however to extrapolate the parton distribution by up to 3 orders in magnitude in Q^2 . This is possible using the pQCD evolution equations. At large x the DGLAP equations are expected to provide a sufficiently good approximation. This is however rather doubtful at small x because terms proportional to $\alpha_s \star \ln 1/x$ have been neglected in the derivation of DGLAP compared to the $\alpha_s \star \ln Q^2$ terms which have been summed. This does not look justified at small x . One important question at HERA is therefore the test of QCD dynamics at small x .

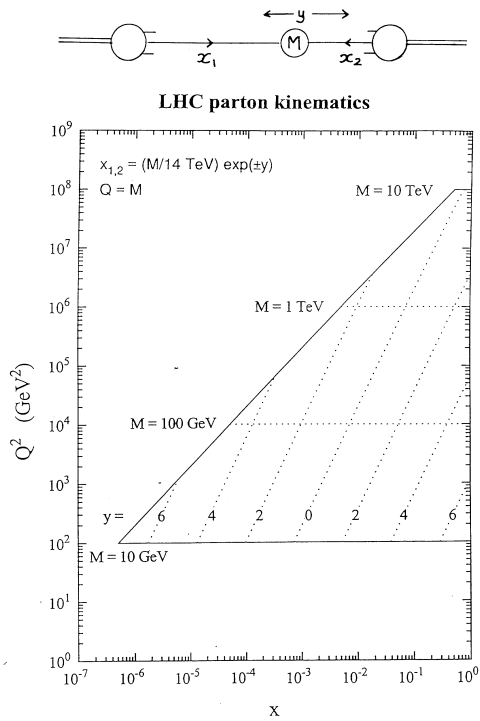


Figure 3: *Kinematic plane of hard scattering processes at LHC. Lines of constant rapidity y for the produced system with mass M are given as dashed lines.*

2 New DIS data

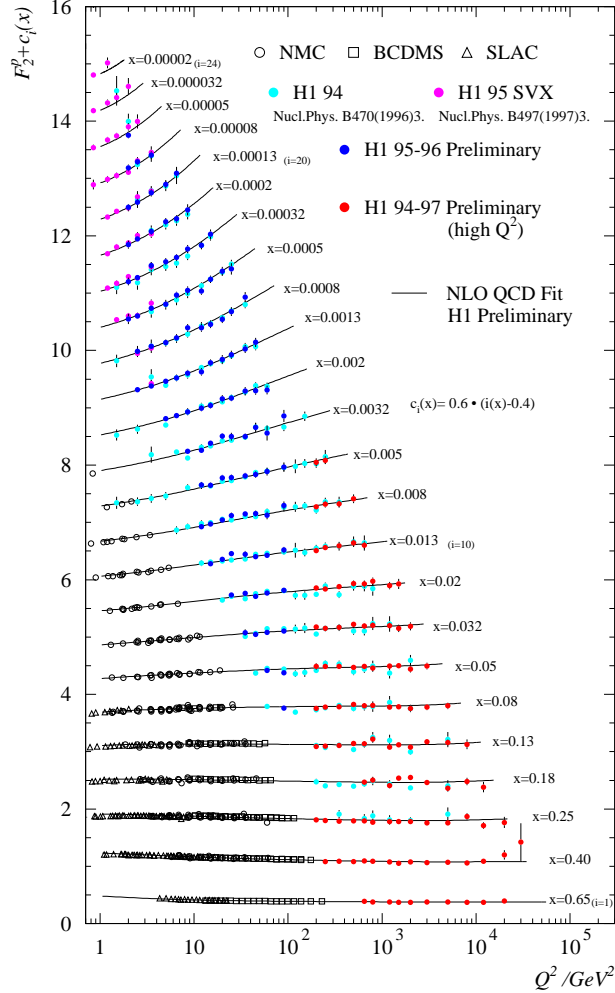


Figure 4: The structure function F_2^{lp} vs. Q^2 for fixed values of x for recent HERA and for fixed target data. The solid lines are the result of a NLO p QCD fit to these data by H1 as discussed below.

Progress in the measurement of nucleon structure functions is steady but rather slow. It takes long time and hard work to make reliable measurements and to study and reduce systematic effects. Nevertheless the best measurements are all dominated by correlated systematic errors which makes it difficult to analyse these data in a consistent quantitative way. From fixed target experiments two important new results have been added. The NMC collabo-

ration has published the final analysis of their data taken back in '89 with a small angle trigger [2]. These data enlarge the low x range and therefore the overlap with HERA and also allow to measure $R = \sigma_L/\sigma_T$. The CCFR neutrino collaboration at Fermilab has published an improved analysis of their data first published in '93 [3]. They have essentially improved the energy calibration for hadrons and muons. Their structure function measurements have a significant impact on our knowledge of α_s , to be discussed at the end. The H1 collaboration has made a very substantial step towards large x and

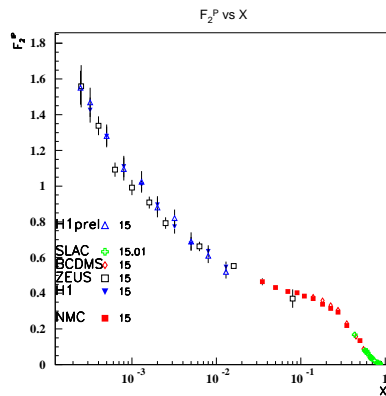


Figure 5: *Fixed target and HERA measurements of F_2^{lp} for a fixed value of $Q^2 = 15 \text{ GeV}^2$.*

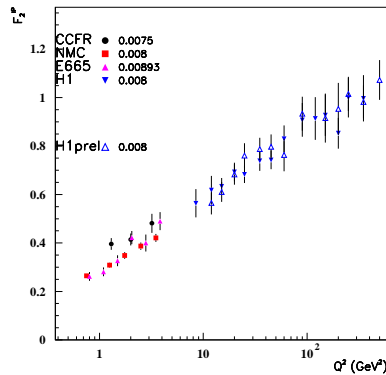


Figure 6: *Fixed target and HERA measurements of F_2^{lp} for a fixed value of $x=.008$.*

Q^2 which allows for the first time to directly test the Q^2 -evolution at large

x over two orders of magnitude with reasonable precision. Also more precise data in the low x region has been provided by both H1 and ZEUS. A compilation of some of the most precise measurements of the structure function F_2^{ep} is shown in figure 4 versus Q^2 for fixed values of x. Figures 5 and 6 show all available data points for a fixed value of $Q^2 = 15 \text{ GeV}^2$ resp. a fixed value of $x=.008$ in order to see the relative precision and the matching of fixed target and HERA data. Figure 5 demonstrates very clearly one of the most important contributions of HERA so far: The structure function at small x and therefore the $q\bar{q}$ sea rises by more than a factor 3 in the HERA range towards small x. This has severely affected the predictions for processes at LHC both for pp and heavy ion collisions. The structure function for fixed $x=.008$ rises by a factor 5 with Q^2 demonstrating huge scaling violations which have to be explained by pQCD. The overall agreement among the two HERA experiments and the matching with fixed target experiments is good. Our knowledge on F_2^{ep} has presently a systematic uncertainty of about $\pm 3\%$ over the whole x-range $10^{-4} < x < .65$ mainly limited by the uncertainties of energy scales.

3 Analysis of the low x region and the gluon distribution

The low x data on F_2 show large scaling violations . For large enough Q^2 these should be described by the pQCD evolution equations:

$$d\Sigma(x, Q^2)/d\ln Q^2 = \alpha_s/2\pi (P_{gq} \otimes g + P_{qg} \otimes \Sigma)$$

$$dxg(x, Q^2)/d\ln Q^2 = \alpha_s/2\pi (P_{gg} \otimes g + P_{qg} \otimes \Sigma)$$

Here $\Sigma = \sum_f x(q_f + \bar{q}_f)$ is the sum of all quark and antiquark momentum distributions. The parton distributions evolve with Q^2 because quarks radiate gluons, gluons split into quark-antiquark pairs and gluons split into gluons. At small x the gluon radiation from quarks can be neglected. The evolution is then dominated by the evolution of the gluon distribution. The splitting functions P_{ij} depend on terms proportional to

$$\alpha_s \star \ln Q^2, \alpha_s \star \ln Q^2 \ln 1/x \text{ and } \alpha_s \star \ln 1/x$$

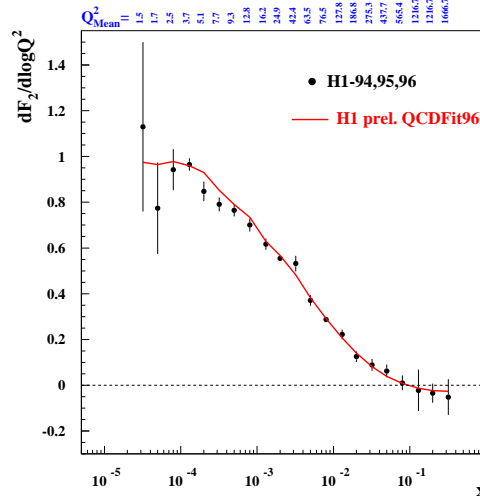


Figure 7: Measured slopes $dF_2/d\ln Q^2$ obtained from linear fits in $\ln Q^2$ to the H1 data. The solid line gives the slopes as obtained from the NLO QCD fit.

If terms proportional $\ln 1/x$ are neglected, then we arrive at the DGLAP evolution equation, if instead terms proportional to $\ln 1/x$ are kept instead of $\ln Q^2$ terms we arrive at the BFKL equation.

The first thing to do is therefore to check the evolution directly. Figure 7 compares the measured slopes $dF_2/d\ln Q^2(x)$ (by linear fits in $\ln Q^2$ for fixed x) with the predictions of a DGLAP fit to the data (H1 fit discussed below). There is good agreement down to $x = 10^{-4}$. This illustrates, to our big surprise, that the DGLAP approximation works even at very small values of x . Other attempts to see 'BFKL' like effects in the final state, which are not discussed here, were also negative.

This observation gives us the possibility to measure the gluon distribution from the measured slopes $dF_2/d\ln Q^2(x)$. To rather good approximation the relation at small x is given by:

$$dF_2/d\ln Q^2(x) \approx 10/27\pi * \alpha_s(Q^2) * xg(2x, Q^2)$$

The HERA experiments therefore measure the gluon distribution at small x which is of prime importance for physics at LHC.

Both HERA collaborations have determined the gluon distribution from a NLO DGLAP fit to their data ($Q^2 > 1.5 \text{ GeV}^2$) in combination with ep and

H1 ($Q_0^2 = 1 \text{ GeV}^2$):

$$\begin{aligned}
 xg(x, Q_0^2) &= A_g x^{B_g} (1-x)^{C_g} \quad \leftarrow 3 \text{ Parameters} \\
 xu_v(x, Q_0^2) &= A_u x^{B_u} (1-x)^{C_u} (1 + D_u x + E_u \sqrt{x}) \\
 xd_v(x, Q_0^2) &= A_d x^{B_d} (1-x)^{C_d} (1 + D_d x + E_d \sqrt{x}) \\
 xS(x, Q_0^2) &= A_S x^{B_S} (1-x)^{C_S} (1 + D_S x + E_S \sqrt{x})
 \end{aligned}$$

- assume $\bar{u} = \bar{d}$
- strange quark 20% of total sea
- $\alpha_s(M_Z) = 0.118$

Figure 8: *Parametrisations of parton momentum distributions as used by H1 and choice of parameters. The solid line gives the slope as obtained from the NLO QCD fit.*

ed data from BCDMS and NMC. This is explained below for the example of H1 [4] which uses 15 free parameters plus some relative normalisation parameters. The resulting gluon distribution is shown in figure 9 at $Q^2 = 20 \text{ GeV}^2$ together with the corresponding determination from ZEUS [4]. The gluon density rises strongly towards small x and $xg(x)$ reaches values of 25 at $x = 10^{-4}$, a factor 15 larger than the sea quark density. This underlines the predominance of the gluon evolution by gluon splitting whereas the splitting of a gluon into a $q\bar{q}$ pair is relatively rare. The error bands given include all known strongly correlated systematic errors. The gluon distribution in the x - range between 10^{-2} and 10^{-4} is therefore known to about 15% from HERA. It should be noted that the charmed quark contribution to F_2 is very substantial (up to 20%) at small x . This contribution is calculated directly in NLO pQCD [5] via the photon gluon fusion process. This contribution has been directly measured by both HERA experiments using DIS events with D^* 's. The preliminary result of ZEUS is shown in figure 10 together with the pQCD prediction based on the gluon distribution of figure 9. There is good agreement showing the consistency of the procedure.

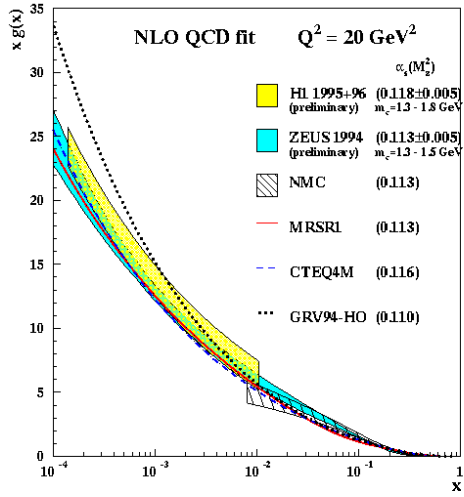


Figure 9: Resulting gluon distribution for $Q_0^2 = 20\text{GeV}^2$ from H1, ZEUS and NMC NLO $p\text{QCD}$ fits. The error bands include the estimate of correlated systematic errors.

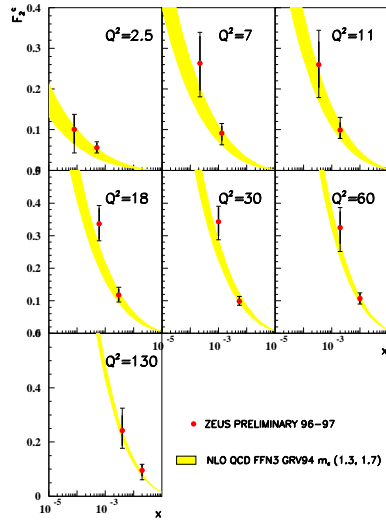


Figure 10: F_2^{charm} as measured by the ZEUS collaboration using D^* production in DIS compared to the NLO prediction based on the γ - gluon fusion process.

4 Transition to low Q^2 at HERA

So far we have discussed the 'DIS-regime' where we believe pQCD is applicable without special justification. It's worthwhile to study the transition region from the DIS regime to the region down to $Q^2 = 0$, e.g. 'photoproduction'. This has been possible at HERA due to the installation of special low angle electron calorimeters which allow to measure inelastic neutral current scattering down to $Q^2 = 0.11 \text{ GeV}^2$ [6]. In addition we can

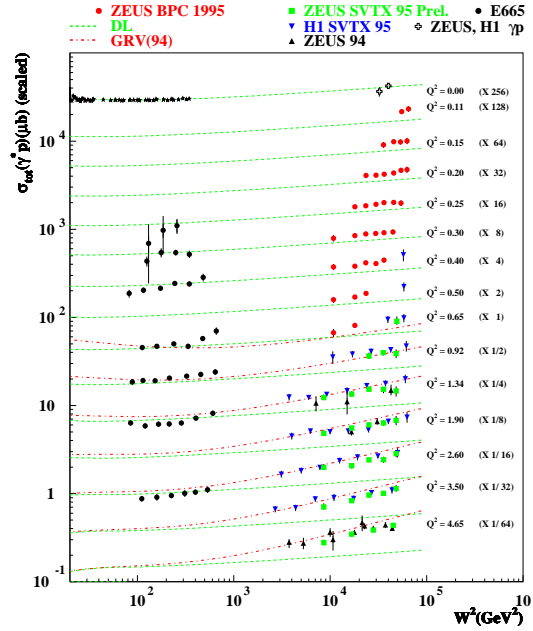


Figure 11: *The total γ^*p cross section vs. W^2 for low values of Q^2 compared to DGLAP (GRV) and soft pomeron regge (DL) predictions.*

of course measure the total photoproduction cross section $\sigma_T^{\gamma p}(W^2, Q^2 = 0)$. The theoretical concepts used to describe DIS and photoproduction can be easily related. The structure function $F_2(x, Q^2)$ and the γp cross section are related by:

$$\sigma_T^{\gamma^* p}(W^2, Q^2) \simeq 4\pi\alpha^2/Q^2 F_2^{ep}(x, Q^2)$$

$$W_{\gamma p}^2 \simeq Q^2/x \text{ at low } x$$

Scattering of electrons at low x is therefore equivalent to high energy γp scattering. Since photons behave like hadrons if they interact with nucleons

it should not be surprising that the concepts which are used to describe high energy hadron-hadron scattering are suitable to discuss the low x region. Figure 11 shows $\sigma_T^{\gamma^*p}$ as function of W^2 for different values of Q^2 . It's well known that the photoproduction cross section has the same rise with W^2 as observed in p-p scattering: $\sigma_T^{\gamma^*p}(W^2, Q^2 = 0) \sim (W^2)^\lambda$ where $\lambda = 0.08$ is the intercept of the 'soft Pomeron trajectory'. The HERA data at low Q^2 show that the increase of σ_T with W^2 becomes larger with increasing Q^2 , therefore λ rises with Q^2 as shown in figure 12 from a value close to .08 at low Q^2 to $\lambda \approx .35$ at $Q^2 = 40 GeV^2$. The measurements are compared to

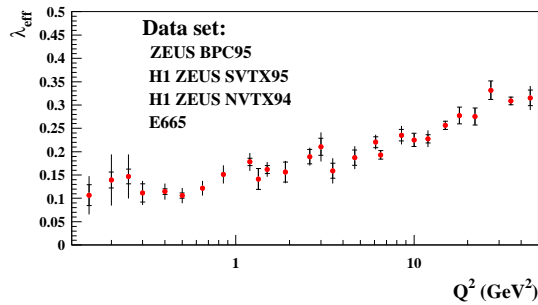


Figure 12: *The exponent λ from a fit $F_2 \sim x^\lambda$ to the H1 data at small x vs. Q^2 .*

a soft pomeron model of Donnachie and Landshoff (DL, dashed curves) and a pQCD fit based on the DGLAP evolution (dash-dotted line). We see a smooth transition from regge models to the DIS description around $Q^2 = .8 GeV^2$. Figure 13 shows another interesting aspect of the transition region. The slopes $dF_2/d\ln Q^2$ have been directly determined from HERA data as a function of x . These slopes rise towards low x from $x = 10^{-1}$ to $x = 10^{-4}$ in agreement with DGLAP predictions given by the triangles but then fall again towards even lower x . The slopes at lowest x are in agreement with regge fits based on the 'soft Pomeron' concept. The transition occurs around $x = 10^{-4}$ at $Q^2 \approx 1 GeV^2$.

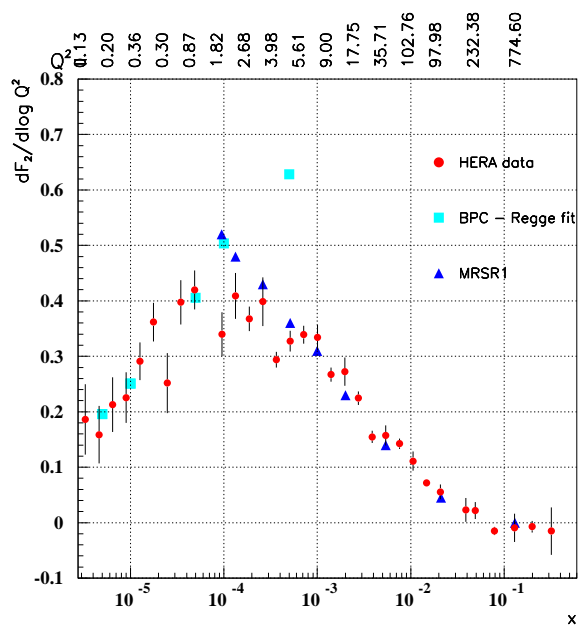


Figure 13: Slopes $dF_2/d\ln Q^2$ measured in the transition region compared to predictions of a DGLAP fit and of a Regge fit.

5 Large x and large Q^2

This is the kinematic region where we want to test the standard model by looking for e.g. contact interactions or new massive particle production (see talk by J. Meyer at this conference). The questions here are;

- how reliable is the standard model prediction e.g. how well can we extrapolate parton densities from fixed target experiments to HERA.
- what are the experimental limitations for a precise measurement at HERA.

The preliminary high x data from H1 is shown in figure 14 where the reduced cross section $\sigma \approx F_2$ up to electroweak interference effects is shown versus Q^2 for different bins in x compared to BCDMS and SLAC data. Also shown

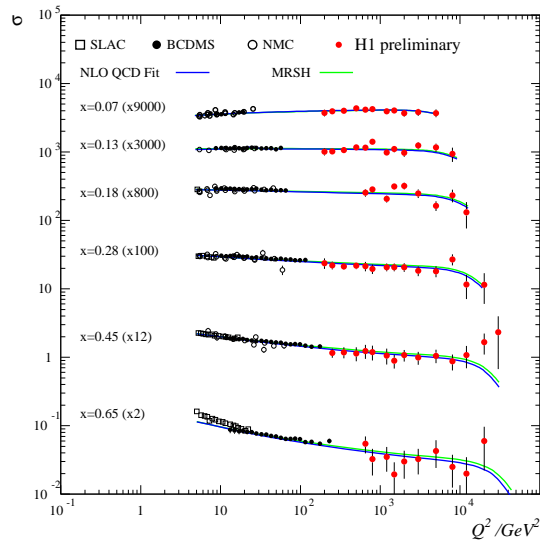


Figure 14: *The reduced cross section for large values of x vs. Q^2 compared to two DGLAP fits to data with $Q^2 < 120 \text{ GeV}^2$ and including the large x data.*

is a QCD fit which used only low Q^2 data. The H1 measurements at an average $\langle Q^2 \rangle = 10000 \text{ GeV}^2$ have an uncertainty of about 14% limited mostly by the uncertainties in the energy calibration. We therefore have so far directly checked the Q^2 evolution over 2 orders of magnitude to that precision. Further improvements will require better calibration in addition to

higher statistics. This is indeed possible at HERA. The energy calibration can be directly obtained from the data by using the redundancy in the kinematic reconstruction. At HERA we measure angle Θ_e and energy E_e of the scattered electron as well as angle Θ_H and energy E_H of the hadronic system (the quark). The energy of the electron can therefore also be calculated from

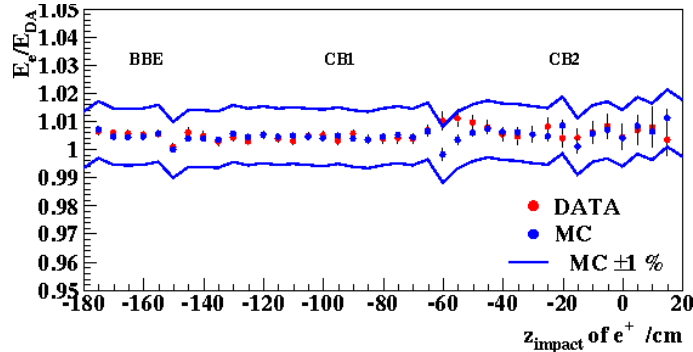


Figure 15: Comparison of the H1 calibration of the electron energy in the liquid argon calorimeter compared to the energy from the double angle method vs. the calorimeter position along the beam axis.

the two angles alone $E_{DA} = f(\Theta_e, \Theta_H)$. The energy scale of the electromagnetic calorimeter vs. polar and azimuthal angle was therefore determined by comparison to the double angle energy. This comparison is shown in figure 15. This procedure determines the energy scale for the scattered electron to about 1% for $\Theta_e > 15^\circ$ and to about 3% for smaller angles where the 3% are limited by statistics.

HERA will substantially increase its luminosity in 2000. High statistics data will then allow better calibration and therefore very good and reliable checks for deviations of the standard model. If a deviation should be observed due to new physics then we are pretty sure that such an effect could be established beyond doubt in contrast to similar measurements at hadron colliders because only quarks can contribute and because the energy calibration is provided by the data themselves.

6 Global fits to parton distributions

The determination of a complete set of parton distributions from available data is the domain of two groups of phenomenologists, the CTEQ group centered at Fermilab and the MRS group at Durham. They provide libraries of particle density functions (PDF) which can be easily used and which are regularly updated if new data become available.

Their global analyses use fit methods very similar to the one described above for H1. They use however additional input in order to also separate the flavour content of valence and sea quarks and to better constrain the gluon distribution. Main additional input comes from the following sources:

- Neutrino measurements from the CCFR collaboration [3] which determine
 - the shape and magnitude of the valence distribution $x(u_v + d_v)$ from the structure function xF_3
 - the magnitude of the strange sea $s(x)/(\bar{u}(x) + \bar{d}(x)) \approx 0.25$ from single charmproduction $\bar{\nu} + \bar{s} \rightarrow \mu^+ \bar{c}$.
 - α_s determination from scaling violations of the nonsinglet structure function.
- Data to determine $u(x)/d(x)$ mostly in the valence region
 - The direct NMC measurement of $u(x)/d(x)$ [7] and the measurement of the asymmetry in W-production by CDF which is the most sensitive measurement at large x [8].
- The determination of \bar{u}/\bar{d} by Drell-Yan experiments
- Experiments measuring direct hard photon production in pN scattering as a direct measurement of the gluon distribution at large x.

No attempt is made here to go into details. Comprehensive summaries can be found in references [9] and [10]. The results which are summarised here in order to illustrate successes and problems of this approach are taken from the recent fit of the MRS group using the PDF set MRS98 [9]. This basic PDF set fixes the value of $\alpha_s(m_Z) = .118$ to the world average.

Global fits have the problem that data sets are incompatible with each other and that practically all data sets are systematically limited with highly

correlated errors. There is no chance to include these errors - even if they would be fully available - into the fits. This may lead to systematic biases of the results and it makes it practically impossible to evaluate reliably the uncertainties of the parton densities.

6.1 DIS data in the global fits

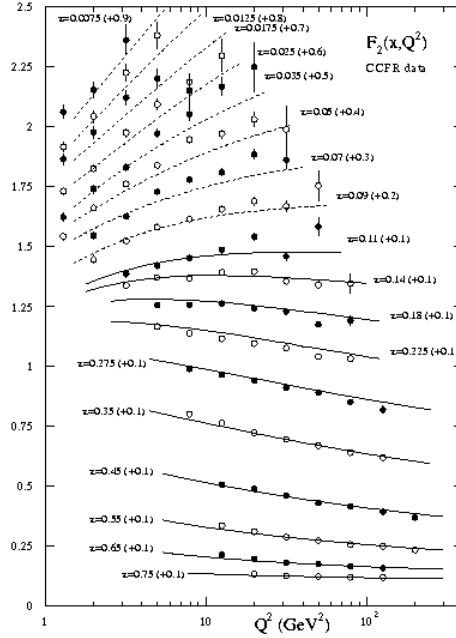


Figure 16: *Measurement of $F_2^{\nu N}(x, Q^2)$ by the CCFR collaboration compared to MRS98 prediction. Only measurements with $x > 0.1$ have been used in the fit.*

There is overall reasonable agreement. Some data sets give rather large contributions to χ^2 / dof like e.g. the BCDMS ep and ed and the ZEUS structure functions but the fits disregard the systematic errors. Both MRS and CTEQ have decided to use single charm production from the CCFR neutrino experiment to fix the strange sea. This however has a problem as illustrated in figure 16. The measured structure function $F_2^{\nu N}$ in the sea region ($x < 0.1$) is 10 % to 20 % higher than expected whereas the NMC muon data is well described. Obviously one has to make a choice and MRS

has decided NOT to use the low x CCFR data in the fit. There is however no explanation for this discrepancy.

6.2 Drell-Yan processes and the \bar{u}/\bar{d} ratio

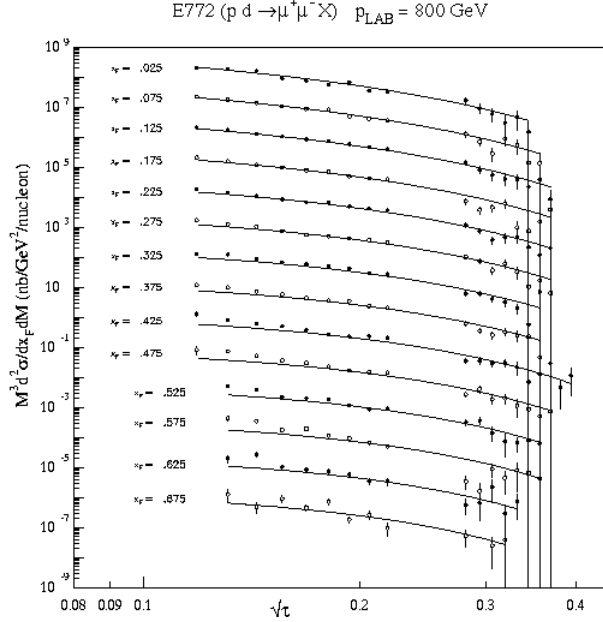


Figure 17: *Drell-Yan cross section of experiment E772 for the process $pd \rightarrow \mu^+\mu^-X$ [11] compared to the NLO predictions based on the MRS98 parametrisation*

Lepton pair production in hadron-hadron scattering outside the Ψ and Y mass ranges as well as the production of the vector bosons at the $\bar{p}p$ collider are rather well described by the Drell-Yan process. Figure 17 shows the differential cross section for the reaction $pd \rightarrow \mu^+\mu^-X$ as measured by the E772 experiment at Fermilab at 800 GeV laboratory energy [11] compared to NLO pQCD predictions based on the MRS98 parametrisation.

The overall agreement is quite good, at a level of about 10%, except in the region of large x_F and small \sqrt{s} where systematic deviations of up to a factor 2 are observed. This region corresponds to scattering processes where the first parton carries a momentum $x_1 \approx 0.4 \div 0.6$ whereas the second parton is at small $x_2 \approx .02$. Both parton densities should therefore be well known

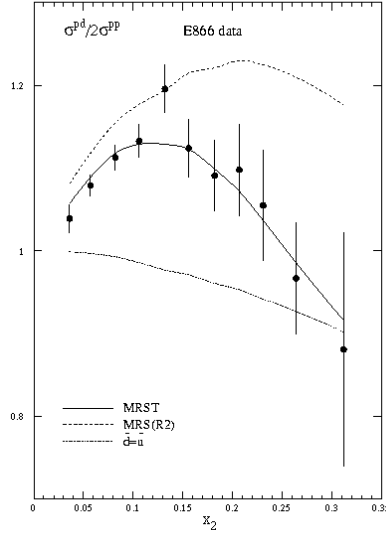


Figure 18: *The cross section ratio $\sigma(pd \rightarrow \mu^+ \mu^- X)/2 \star \sigma(pp \rightarrow \mu^+ \mu^- X)$ as measured by experiment E866 [13] compared to predictions based on $\bar{u}/\bar{d} = 1$. and on the MRS98 PDF with $\bar{d} > \bar{u}$*

such that the origin of the discrepancy is either an experimental problem or a problem in the theoretical calculation.

If one disregards this kind of problems then Drell-Yan data can be used to measure the flavour content of the sea quarks especially the \bar{u}/\bar{d} ratio. We know for quite some time that there are more down quarks in the sea than up quarks because the Gottfried sum rule as measured by NMC [7]

$$\int_0^1 (F_2^{\mu p} - F_2^{\mu n}) dx/x = 1/3 - 2/3 \int_0^1 (\bar{d} - \bar{u}) dx = .235 \pm .026$$

differs significantly from 1/3 and because the Drell-Yan experiment NA51 measured $\bar{d}/\bar{u} > 1$ at $x \approx .5$ [12]. A new dedicated experiment (E866) at Fermilab has made very precise measurements in '97 to clarify this question [13]. E866 measured the cross section ratio $\sigma(pd \rightarrow \mu^+ \mu^- X)/2 \star \sigma(pp \rightarrow \mu^+ \mu^- X)$ directly which depends on \bar{d}/\bar{u} . This cross section ratio is shown in figure 18 versus x compared to predictions for $\bar{d}/\bar{u} = 1$. The MRS98 fit uses this data to fix the flavour ratio of the sea quarks.

The measured difference between down and up quarks in the sea is well compatible with models where the nucleon has a pion cloud.

The ratio of up and down quark densities at large x e.g. in the valence

region can be derived from $F_2^{\mu n}/F_2^{\mu d}$ as measured by NMC [7]. A very sensitive new measurement at high scale has been provided by CDF [8] which measured the asymmetry of the decay leptons from W^\pm bosons at the $\bar{p}p$ collider. This measurement has been selected by MRS to determine u/d in the valence region together of course with the BCDMS structure function measurements on proton and deuterium.

6.3 Measurement of the gluon distribution

The gluon distribution is notoriously difficult to measure over the whole x range. In the small x region ($x \leq .1$) the gluon distribution is reasonably well measured from $dF_2/d\ln Q^2$ by the HERA experiments and NMC as described above. This does not help at larger x because there the scaling violations due to quarks radiating gluons dominate over the gluon splitting contribution. A very strong constraint for the gluon distribution at medium and large x is however given by the energy momentum sum rule.

A direct measurement of the gluon distribution at medium and large x is very desirable. The best suited process is direct hard photon production in pN scattering. This process in leading order is absolutely dominated by quark-gluon scattering, $q\bar{q}$ processes give a relatively small and well known contribution. Very precise new measurements for this process over a large kinematic range have been provided by experiment E706 [14] as shown in figure 19. The invariant cross section for the process $pBe \rightarrow \gamma X$ at 530 GeV and 800 GeV has been measured for transverse momenta of the photon between 3.5 and 11 GeV/c which covers a range of the gluon fractional momentum $.3 < x_\gamma < .5$. The NLO pQCD prediction based on the 'canonical' gluon distribution is unable to describe this data, it is about a factor 2 too low. The pQCD predictions have a rather large scale dependence; what is however worst is the fact that single photon production requires a large 'intrinsic' $k_T \approx 1$ GeV/c of the incoming gluon as e.g. shown by the imbalance of photon and jet momenta of $\gamma - jet$ events. Adding a value of $k_T = 1$ GeV/c changes the cross section by about a factor 2 independent of p_T [14]. Both observations show that the theoretical understanding of this process is not sufficient and as long as this does not change this process cannot be used to rigorously constrain the gluon distribution at large x . This is

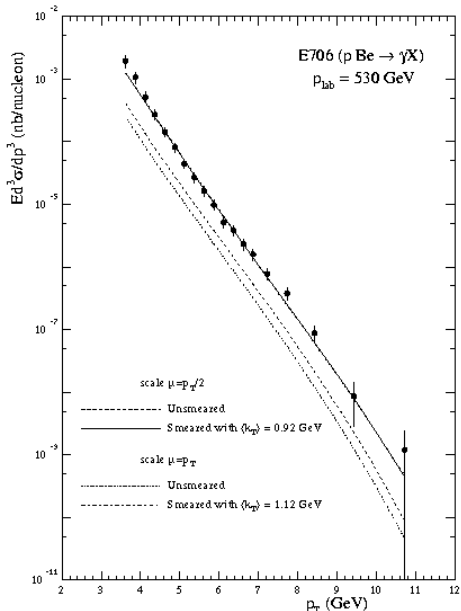


Figure 19: *The single photon cross section as measured by experiment E701 in pBe interactions at 530 GeV. The different curves give NLO predictions based on MRS98 using two scales and adding an intrinsic $k_T = 1.2$ GeV.*

rather unfortunate because these measurements can in principle decide between conventional and 'unconventional' shapes of the gluon distribution at large x which have been proposed to explain the excess of dijet events by CDF [15] .

6.4 How well do we know the parton distributions?

The parton momentum distributions from the MRS98 fit are shown in figure 20 for a scale $Q^2 = 20 \text{ GeV}^2$. These can be used to predict hard scattering processes. The question of course is: what are the errors for such a prediction. This information is not really available. The procedure to estimate this error by comparing different parton density parametrisations which can be found rather often is completely inadequate. It happens too often that the addition of new data changes the PDF data sets far outside the error estimates given before. Examples of recent changes are given in figure 21 taken from the last MRS global fit paper [9].

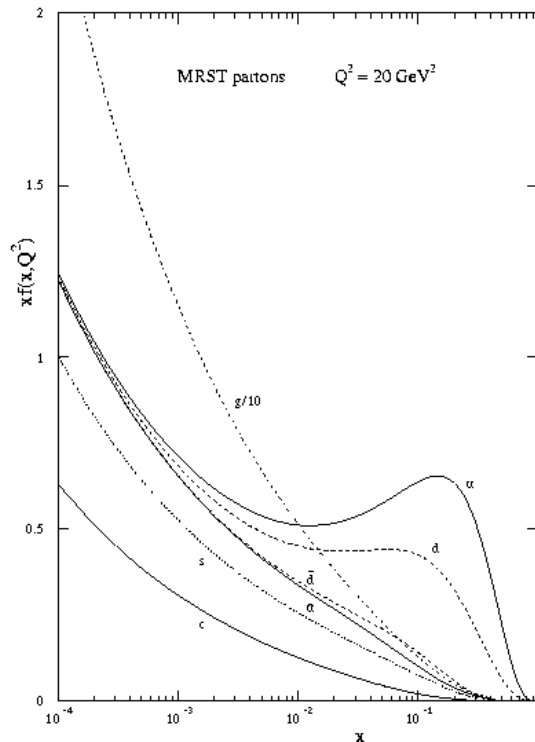


Figure 20: *Parton momentum distributions for a scale $Q^2 = 20\text{GeV}^2$ for the MRS98 fit [9].*

It shows the relative changes for valence quarks and gluons for the MRS global fits of '97 and '98. Most surprising is the change of the down quark density at large x by up to 25 %. This is the result of including the CDF W^\pm asymmetry measurements in the fit.

The knowledge of parton distributions is experimentally limited by the fact that practically all data sets are dominated by systematic errors where calibration errors are dominant. Different data sets also show inconsistencies, such that we have to make a choice which ones to use. New data alone will not be sufficient to make progress. We need a better treatment of systematic errors in the fits where possible and we have to be more selective in choosing the data sets entering the fits. Those parts of data sets which have large correlated systematic errors should be disregarded in future.

On the theoretical side more studies are needed to see if the parametrisations have enough flexibility. NNLO calculations for DIS would be welcome

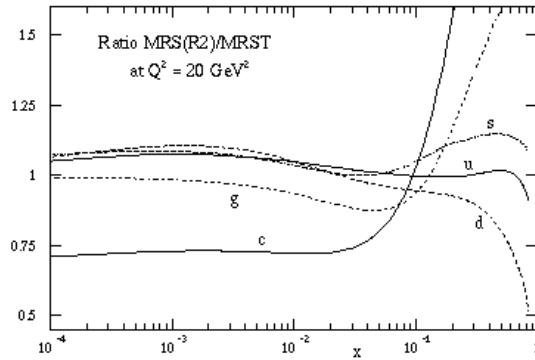


Figure 21: *Relative changes of parton densities vs. x for MRS fits from '97 and '98.*

in order to reduce the scale dependences. Most of all we need however a satisfactory theoretical description of single photon production to nail down the gluon distribution at large x .

Our knowledge of parton densities to my personal judgement can be roughly summarised as follows

- the cross sections for qq and $q\bar{q}$ processes can be predicted with an error $\Delta\sigma/\sigma \leq 10\%$ for $10^{-4} < x < .3$. The error increases to about 20 % for larger values of x .
- for gluon-gluon scattering we have $\Delta\sigma/\sigma \leq 20\%$ for $x < .1$. The error increases to 30% up to $x=.3$ and is about 60% for $.3 < x < .4$. These error estimates are more conservative than what is normally given by the authors of PDF's.

Experimental improvements can be expected from HERA in future for quarks and gluon densities at small x with better statistics and improved systematic understanding of the detectors.

6.5 Determination of α_s from DIS.

The uncertainty of α_s gives a non negligible contribution to our knowledge of parton densities at high scales. The strong coupling constant α_s can be well determined from the observed scaling violations in DIS because the pQCD prediction does not suffer from large theoretical uncertainties and because experimental errors are also small. Since several years the world average of α_s from DIS experiments was always quoted to be low compared to LEP measurements. It should be noted that this low value of α_s was enforced by only two experiments: the BCDMS muon experiment which published a value $\alpha_s(m_Z) = .113 \pm .003_{exp} \pm .004_{th}$. [16] and by the CCFR neutrino experiment which in '93 published a value $\alpha_s(m_Z) = .111 \pm .002 \pm .003_{syst}$ [17] The CCFR collaboration has recently published a reanalysis of the same data [3]. After significant improvements of the calibration for hadrons and muons the old published value is changed to $\alpha_s(m_Z) = .119 \pm .002_{exp} \pm .004_{th}$. This leaves BCDMS as the sole data set which requires a small value. Its worth while to have a closer look to this data. The large x data for F_2^{ed} from

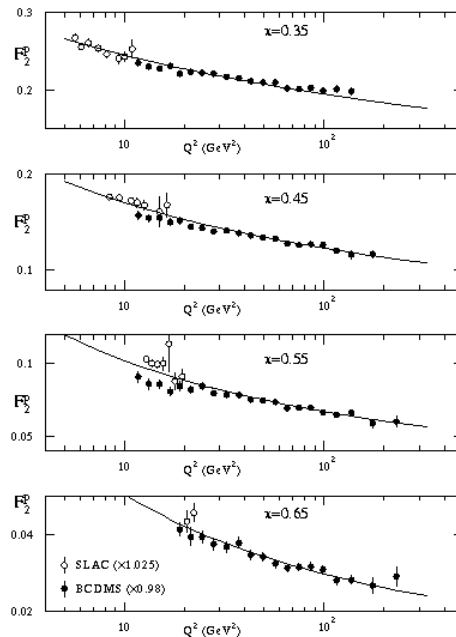


Figure 22: *The measurements of $F_2^{\mu d}$ at large x from BCDMS compared to neighbouring data points from SLAC and the MRS98 fit with $\alpha_s = .118$.*

BCDMS is shown in figure 22 together with SLAC data and a global QCD fit with $\alpha_s = .118$. For each x bin the data points at low Q^2 show large and very significant deviations from the fit curve but also from the SLAC data points leading to a very poor $\chi^2/dof = 248/174$. The data points with systematic deviations are at low y where every DIS experiment has the most serious systematic problems due to energy calibration. This is also clearly stated in the BCDMS paper [18] which says: ..” the data agree with SLAC within the large correlated systematic errors..”. A fit which uses these statistically very precise data points disregarding the systematic errors will therefore severely bias the result and necessarily lead to wrong results.

My conclusion is that i) DIS data is in agreement with a world average of $\alpha_s \approx .118$ and ii) people which make global fits for PDF determination should care more about systematics, best in collaboration with experimentalists.

References

- [1] J. Stirling, Parton distributions and the LHC, presented at the theory of LHC processes workshop, febr. 9-13 (1998)
<http://wwwth.cern.ch/lhcworkshop98/ps/program.html>
- [2] M. Arneodo *et al.*, Nucl. Phys. **B483** ,(1997) 3.
- [3] W.G. Seligman *et al.*, Phys. Rev. Lett. **79**, (1997) 1213.
- [4] H1 collab., Paper 262 presented at HEP97 conference, Jerusalem, 1997.
M.A.J. Boje, Proceedings of 5th International Workshop on DIS and QCD, Chicago April 14-18 1997.
- [5] S. Riemersma *et al.*, Phys. Lett. **B347** (1995) 143.
- [6] J. Breitweg *et al.* , hep-ex/9707025, Phys. Lett. **B407** (1997) 432.
- [7] P. Amaudruz *et al.*, Phys. Rev. Lett. **66** (1991) 2712.
- [8] A. Bodek, Acta Phys. Polon. **B28** (1997) 477.
- [9] A.D. Martin *et al.*, ”Parton distributions: a new global analysis”, hep-ph/9803445.

- [10] H.-L. Lai *et al.*, Phys. Rev. **D55** (1997) 1280.
- [11] P.L. Gaughey *et al.*, Phys. Rev. **D50** (1994) 3038.
- [12] A. Baldit *et al.*, Phys. Lett. **B332** (1994) 244.
- [13] E.A. Hawker *et al.*, hep-ex/9803011, to be published in Phys. Rev. Lett.
- [14] L. Apanasevich *et al.*, hep-ex/9711017.
- [15] J. Houston *et al.*, hep-ph/9511386.
- [16] M. Virchaux and A.M. Milsztajn, Phys. Lett. **B274** (1992) 221.
- [17] P.Z. Quintas *et al.*, Phys. Rev. Lett. **71** (1993) 1307.
- [18] A.C. Benvenuti *et al.*, Phys. Lett. **B237** (1990) 592.